Application of the ADS method to predict a "hidden" basal detachment: NW Borneo fold-and-thrust belt

Filippo Carboni[a,*], Stefan Back[b], Massimiliano R. Barchi[a]

[a] GSG – Department of Physics and Geology, University of Perugia, Via Alessandro Pascoli, 06123, Perugia, Italy
[b] Geologisches Institut, RWTH Aachen University, Wüllnerstr, 252056, Aachen, Germany

ABSTRACT

The NW Borneo margin is characterized by a complex deepwater fold-and-thrust belt. Despite previous studies, the definition of a univocal detachment level for folding and thrusting is still lacking. The area-depth-strain (ADS) method can be used to determine the location for a detachment in areas lacking data, and to balance geological cross sections. This study applies the ADS method to the central part of the NW Borneo fold-and-thrust belt to predict a structurally conclusive detachment level in an area lacking a seismic detachment reflection.

Seismic interpretations were completed after the ADS-determination of the basal detachment, providing input for a 2D sequential restoration that delivered values on shortening distribution and shortening rate. The kinematic and mechanic analyses presented, document that the central part of the NW Borneo fold-and-thrust belt is affected by both, near- and far-field stresses, and that the far-field crustal shortening component becomes more important northward. This work demonstrates that the ADS method can be effectively applied in fold-thrust belt settings with limited information on the detachment, supports in a quantitative way the tectonic and stratigraphic interpretation of seismic-reflection data and provides a robust structural base for the restoration of balanced cross-sections, including the reconstruction of syn-kinematically eroded stratigraphy.

1. Introduction

The tectonic interpretation of the subsurface structures of fold-and-thrust belts (FTBs) worldwide is largely based on seismic-reflection data. In most cases, seismic-reflection data can effectively constrain the near-surface geometry of folds and thrust faults, but often fails to clearly image the roots of fold-thrust systems because of e.g. subsurface energy loss due to steeply dipping structural and lithological boundaries, significant lateral and vertical rock inhomogeneities, stratigraphic repetition accompanying thrusting, and/or the general deterioration of the seismic signal with depth. Therefore several methods have been developed to determine the depth to detachments, many of which are based on near-surface geometric analysis and area balancing. Pioneering work by Chamberlin (1910) was followed by many other authors, including in recent times the area-depth-strain (ADS) method (Epard and Groshong, 1993; Groshong, 1994, 2015; Groshong et al., 2012; Schlische et al., 2014), the thickness-relief method (Hubert-Ferrari et al., 2005; Gonzalez-Mieres and Suppe, 2006) and the fault-trajectory method (Eichelberger et al., 2017). Wang et al. (2017) recently improved the ADS method to be applied to fold-thrust systems with wedge-shaped layers overlying a dipping, bed-parallel detachment.

This work applies the ADS method sensu Wang et al. (2017) to the central part of the deepwater NW Borneo FTB. This FTB is characterized by an inner extensional domain and an outer compressional domain; this study focuses on the latter. In deepwater NW Borneo FTB, most previous studies have interpreted – at varying depths – a southeast-dipping regional detachment (Hinz et al., 1989; Franke et al., 2008; Hesse et al., 2009, 2010a, 2010b; Cullen, 2010; King et al., 2010a; Sapin et al., 2011, 2013). The presence, below the outer part of the wedge (i.e. to the northwest), of a strong reflection between 5 and 6 km b.s.l., interpreted as a detachment level, represents a good starting observation to speculate about the possible depth and geometry of the detachment towards the southeast, where it is more difficult to determine the depth to detachment for most of the seismic lines. Therefore, an unambiguous, generally accepted interpretation of the exact detachment location, geometry, depth and dip is still lacking. Previous tectonic restorations of the compressional domain (e.g. Hesse et al., 2009; King et al., 2010a) are limited to fold and thrust-fault balancing focusing on depths significantly above a suspected, yet seismically unresolved detachment level. To overcome this limitation, we use the ADS method to quantitatively constrain the depth and geometry of the

* Corresponding author.
  E-mail addresses: filippo.carboni@studenti.unipg.it (F. Carboni), back@geol.rwth-aachen.de (S. Back), massimiliano.barchi@unipg.it (M.R. Barchi).

basal detachment along four representative seismic-reflection profiles recorded by the German Federal Institute for Geosciences and Natural Resources (BGR) in 1986, which were re-processed and depth migrated in 2006 (Hesse et al., 2009). The detachment depth obtained by applying the ADS method is then compared with previous interpretations based on 2001 seismic-reflection data of Franke et al. (2008) and on the detachment suggested by Cullen (2010), and with the relationship between the fault-related anticlines wavelength and the stratigraphic thickness following Morley et al. (2011). The detachment depth predicted by the ADS method was furthermore used to interpret the kinematics of the compressional domain of the NW Borneo FTB, particularly focusing on i) reconstructing the shortening distribution and ii) discussing the relationships between present-day, short-term shortening rates measured by GPS (Rangin et al., 1999; Simons et al., 2007; Sapin et al., 2013) and long-term shortening measured by our tectonic restoration. We finally analyze the reconstructed wedge-taper angles by applying the classical critical wedge theory (Davis et al., 1983; Dahlen, 1990) and the FTB classification approach by Morley et al. (2011).

2. Geological framework

Borneo is a part of Sundaland, which is considered to be a SE Asia promontory of the Eurasia Plate (Fig. 1). Borneo is surrounded by the South China Block in the north, Cenozoic subduction zones along the boundary to the Philippine Sea Plate in the east, and the Indian-Australian Plate in the south and west (Hall et al., 2008). The evolution of the South China Sea during Oligocene – Early Miocene times (Hinz et al., 1989) controlled the formation of the NW Borneo continental margin. Seafloor spreading of the South China Sea led to a southeastward rifting of thinned continental crust of the Dangerous Grounds (e.g. Hamilton, 1979; Holloway, 1981; Taylor and Hayes, 1983; Hinz and Schlüter, 1985; Briais et al., 1993; Barckhausen and Roeser, 2004),

and to the subduction of an older oceanic crust region, the Proto-South China Sea (Hinz et al., 1989; Hall, 1996; Morley, 2002; Hall et al., 2008), beneath NW Borneo. Continental crust of the Dangerous Grounds entered the subduction zone in Early Miocene times, until around 20 Ma, when its buoyancy progressively slowed down and finally locked the system (James, 1984; Levell, 1987; Hinz et al., 1989; Hazebroek and Tan, 1993; Hutchison, 1996; Hall, 1996; Sandal, 1996; Milsom et al., 1997). This collision led initially to the deformation of onshore late Early Miocene sedimentary units (e.g. Tongkul, 1994; Sandal, 1996; William et al., 2003), followed by folding of onshore and shelfal Middle to Late Miocene sedimentary units, and folding and thrusting of Late Miocene to present-day slope sequences (e.g. Levell, 1987; Hinz et al., 1989; Hazebroek and Tan, 1993; Morley et al., 2003; Ingram et al., 2004; Morley, 2009; Hesse et al., 2009).

On the NW Borneo continental slope, the seafloor expression of several thrust-related anticlines records the ongoing deformation (Hinz et al., 1989; Morley, 2007, 2009; Hesse et al., 2009; 2010a, b). The origin of deformation is still a matter of debate, and different causative mechanisms have been proposed: i) reactivation of the old subduction zone beneath NW Borneo (as a zone of weakness) induced by far-field stresses from the Indian-Australian plate and Philippine plate subduction zones, as well as from deformation around Sulawesi (e.g. Hinz et al., 1989; Hall, 2002); ii) gravitational delta tectonics (e.g. Tan and Lamy, 1990; Hazebroek and Tan, 1993; Hutchison, 2004); iii) Hesse et al. (2009) suggested that in the southern part of NW Borneo, modern shelfal growth acts as primary control for gravity-driven shortening, while in the northern part shortening reflects Pliocene to recent deep-rooted, collision-related basement tectonics; iv) gravitational collapse of the uplifted ranges during Miocene to recent times, caused by mantle processes underlying northern Borneo, inducing folding and thrusting with northwestern vergence (e.g. King et al., 2009; Morley et al., 2011; Sapin et al., 2012; Hall, 2013). Even neo-tectonic studies, mostly based
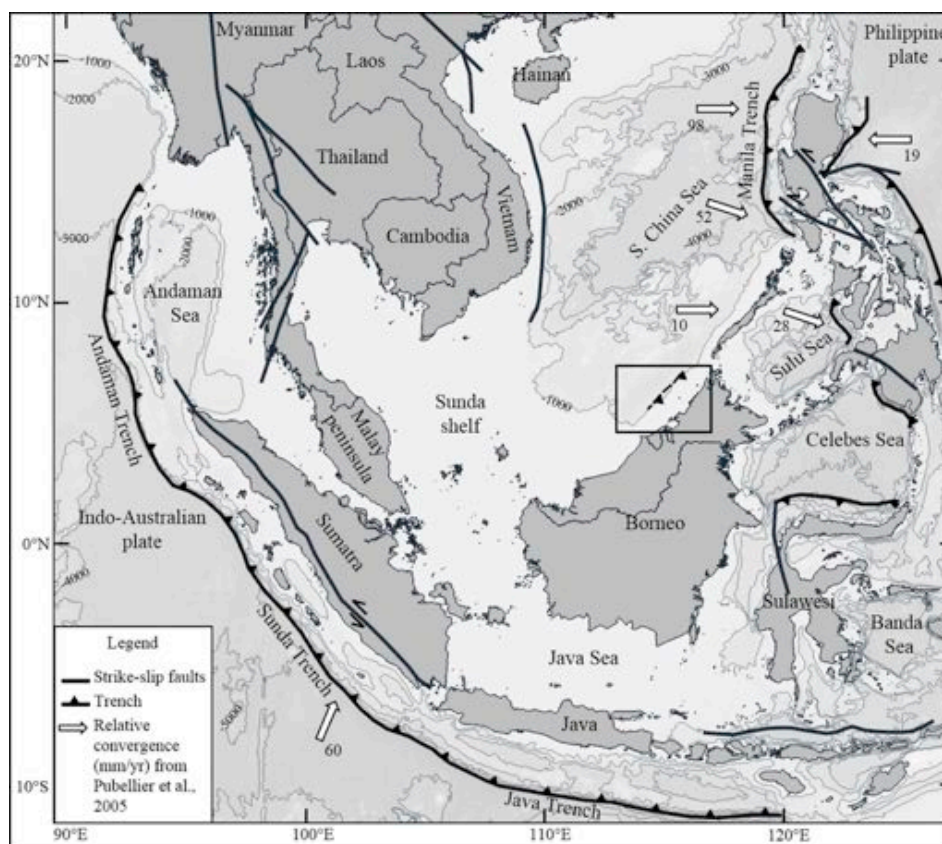

Fig. 1. Main geological features of the SE Asia region and location of the NW Borneo study area (black box). The Sunda Shelf is shaded in white.

on geodetic data, are still a matter of debate. GEODYSSEA GPS data have been interpreted to document a present-day westward motion of NW Borneo respect to a Sunda Block, at the rate of ~11 mm/yr (Rangin et al., 1999). Simons et al. (2007) proposed a significant amount of the shortening produced by the westward motion of NW Borneo at a rate between 4 and 6 mm/yr, accommodated by an active NW Borneo Trench. Sapin et al. (2013), redefining the local reference frame using GPS stations unaffected by internal deformation of NW Borneo, suggested the NW Borneo coastal area - independently of the rest of the island – is moving to the NW at a rate of ~3 mm/yr, and attributed this to large-scale, gravity sliding phenomena (see also Hall, 2013). Mustafar et al. (2017) interpreted continuous GPS data from the International Global Navigation Satellite System Service (IGS) and concluded that gravity sliding alone, along the NW Borneo coastal zones, could not explain the observed deformation and suggested that recent gravity-sliding is co-acting with deep-seated crustal shortening. All these GPS-based reconstructions should be considered in comparison with the results by Hesse et al. (2009), who showed by tectonic restoration that far-field stresses acted and prevail mainly in the northern part of NW Borneo with a SE-NW directed principal compression direction.

3. Seismic data

3.1. Acquisition and processing

The acquisition of the 3129 km of 2D multichannel reflection seismic data used in this study was performed using a 3000 m long digital streamer (4 ms sample rate, 12 s record lengths, 27 lines). In 2006, lines BGR86-18, BGR86-20, BGR86-22 and BGR86-24, interpreted in this work (Fig. 2), were reprocessed, performing a spherical divergence correction, muting, filtering, interactive velocity analysis, and a post-stack depth migration. NMO-correction and stacking followed a pre-stack process in which a radon velocity filter with an inner trace mute provided a sufficient multiple suppression. The velocity model used for the post-stack depth migration was estimated from the stacking velocities determined by semblance analysis and converted into interval velocities using a smoothed-gradient algorithm. An implicit finite difference (FD) migration code, used to obtain the final depth migration algorithm, was run for quality control of the post-stack depth migration. All seismic data presented in this paper are from the 2006 reprocessing series (Hesse et al., 2009) and displayed with no additional gain applied and with a mute above the sea bottom.

3.2. Seismic interpretation

The seismic interpretation used in this work is based on previous interpretations (Hinz et al., 1989; Franke et al., 2008; Hesse et al., 2009, 2010a,b; King et al., 2010a,b; and Sapin et al., 2011, 2013). The stratigraphic subdivision comprises five seismic units (U1 to U5) bound by five seismic horizons (H1 to H5, bottom to top) using relative ages from Hesse et al. (2009, 2010a, b). The interpretations of seismic-reflection lines BGR86-18 (north) to BGR86-24 (south; locations in Fig. 2) are shown in Fig. 3 (BGR86-18), Fig. 4 (BGR86-20), Fig. 5 (BGR86-22) and Fig. 6 (BGR86-24).

On all lines, seismic horizon H1 is a positive, high amplitude reflection, continuous in the most basinward part of the data in depths between 6 and 8 km. Seismic unit U1, bound by H1 at the top,
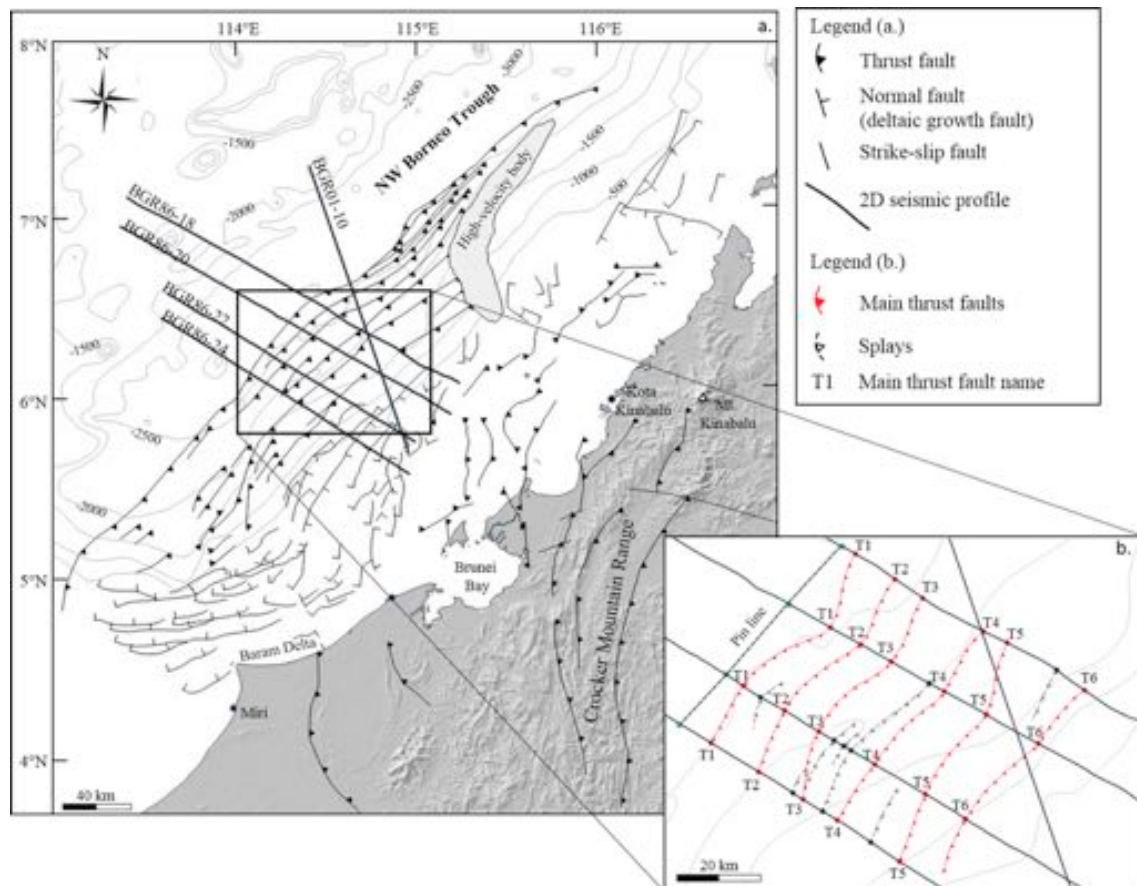

Fig. 2. (a.) Tectonic map of the NW Borneo area showing the main structural elements and the location of the seismic profiles interpreted in this work (modified after Hesse et al., 2009). (b.) Zoom at the compressional area interpreted in this work. The main thrust faults of each section are named sequentially toward the hinterland; the thrust faults trajectories, obtained by joining the fault tips of similar tectonic elements, strike NE-SW.
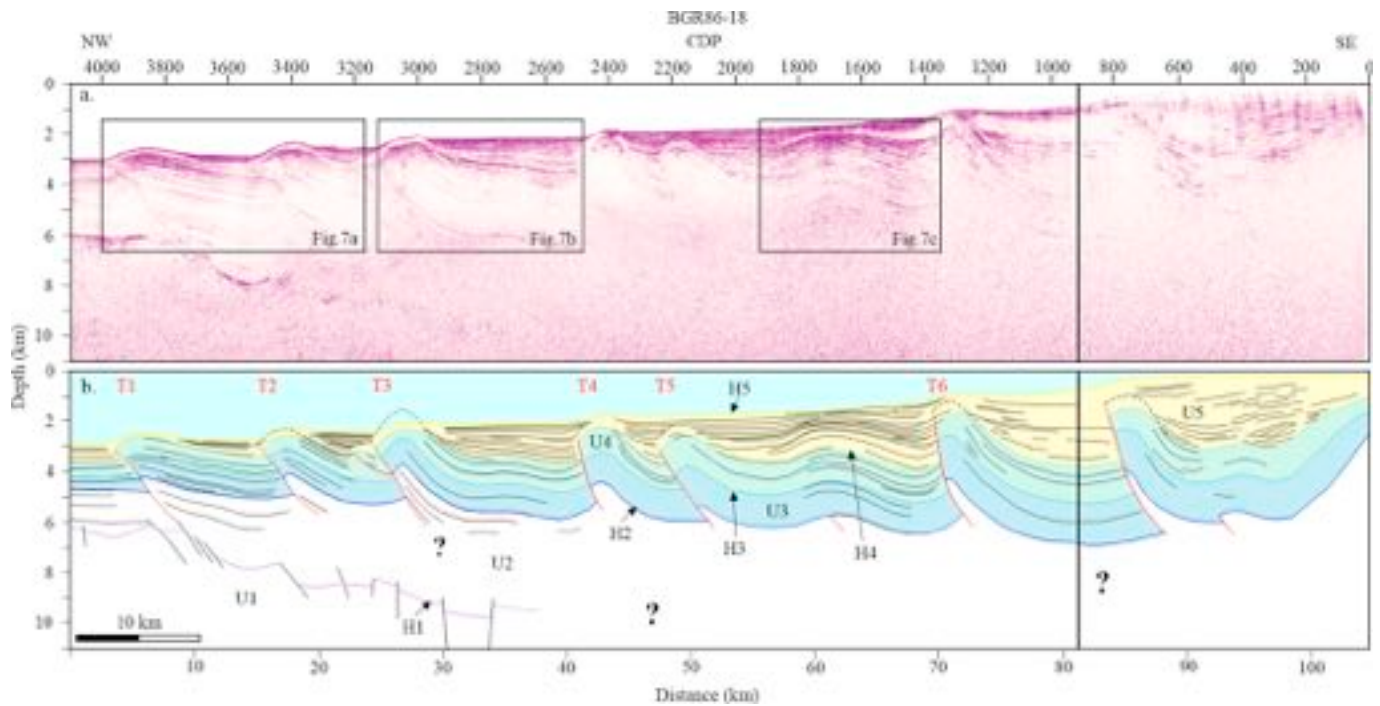
Fig. 3. (a) Uninterpreted seismic profile BGR86-18. (b) Initial interpretation of the seismic profile displaying the seismic units (U) and the seismic horizons (H). Names of the main thrust faults are labeled in red. Vertical exaggeration x2.

represents the acoustic basement, which is characterized by chaotic reflections. In places, reflections of the acoustic basement are offset by normal faults forming horst and graben systems filled with onlapping discontinuous, medium-amplitude reflections. Landwards the detectability of seismic horizon H1 generally decreases.

Seismic horizon H2 is of medium to high amplitude, continuous, and best recorded in the western, seaward parts of the seismic data. Seismic unit U2 below H2 is of an inferred Early to Late Miocene age (Hesse et al., 2009, 2010a; b). This unit is characterized by continuous,

sub-parallel, low to medium amplitude reflections. Within U2 the seismic signal strength decreases both with depth and landwards.

Seismic horizon H3 follows a continuous, low to mid amplitude reflection; seismic unit U3 below has an inferred Late Miocene age (Hesse et al., 2009, 2010a; b) and is characterized by sub-parallel, continuous low to medium amplitude reflections.

Seismic horizon H4 is a prominent reflection that can be identified on all seismic lines as a high amplitude reflection of high continuity. It is considered as an unconformity of Pliocene age (~3.6 Ma, Franke
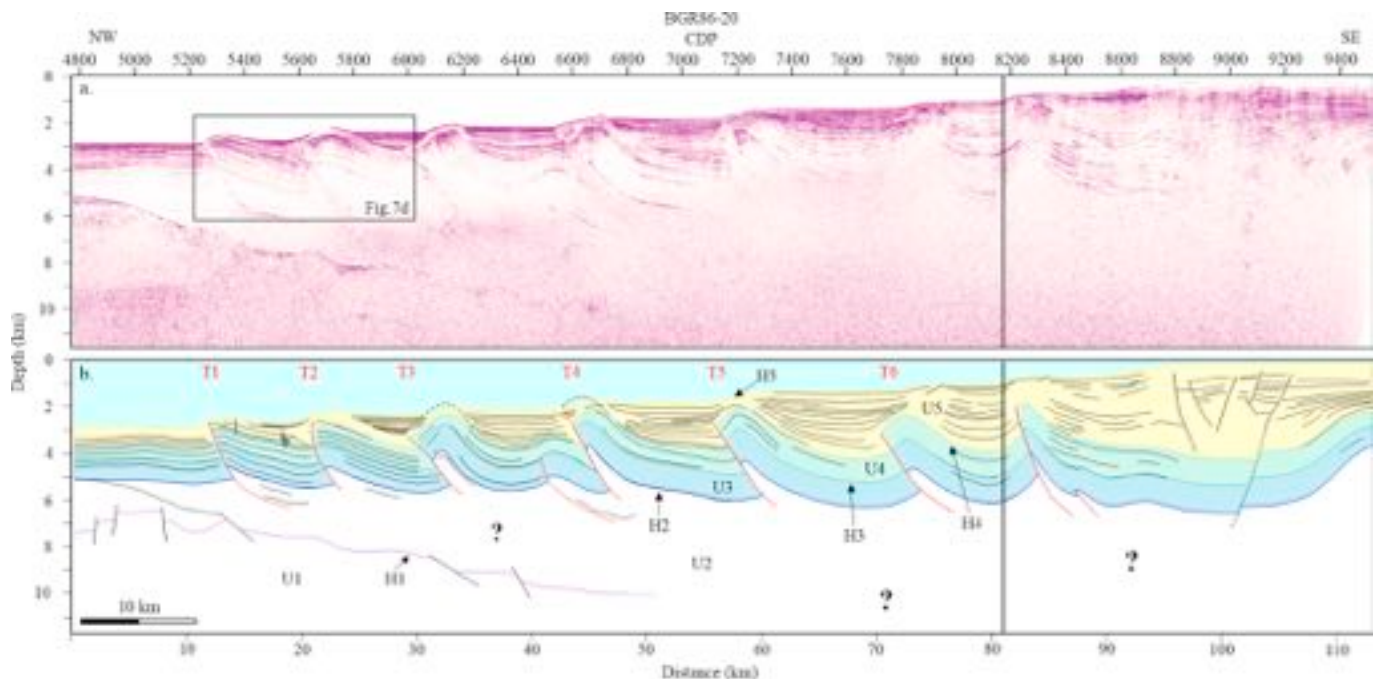

Fig. 4. (a) Uninterpreted seismic profile BGR86-20. (b) Initial interpretation of the seismic profile displaying the seismic units (U) and the seismic horizons (H). Names of the main thrust faults are labeled in red. Vertical exaggeration x2.

Fig. 5. (a) Uninterpreted seismic profile BGR86-22. (b) Initial interpretation of the seismic profile displaying the seismic units (U) and the seismic horizons (H). Names of the main thrust faults are labeled in red. Vertical exaggeration x2.
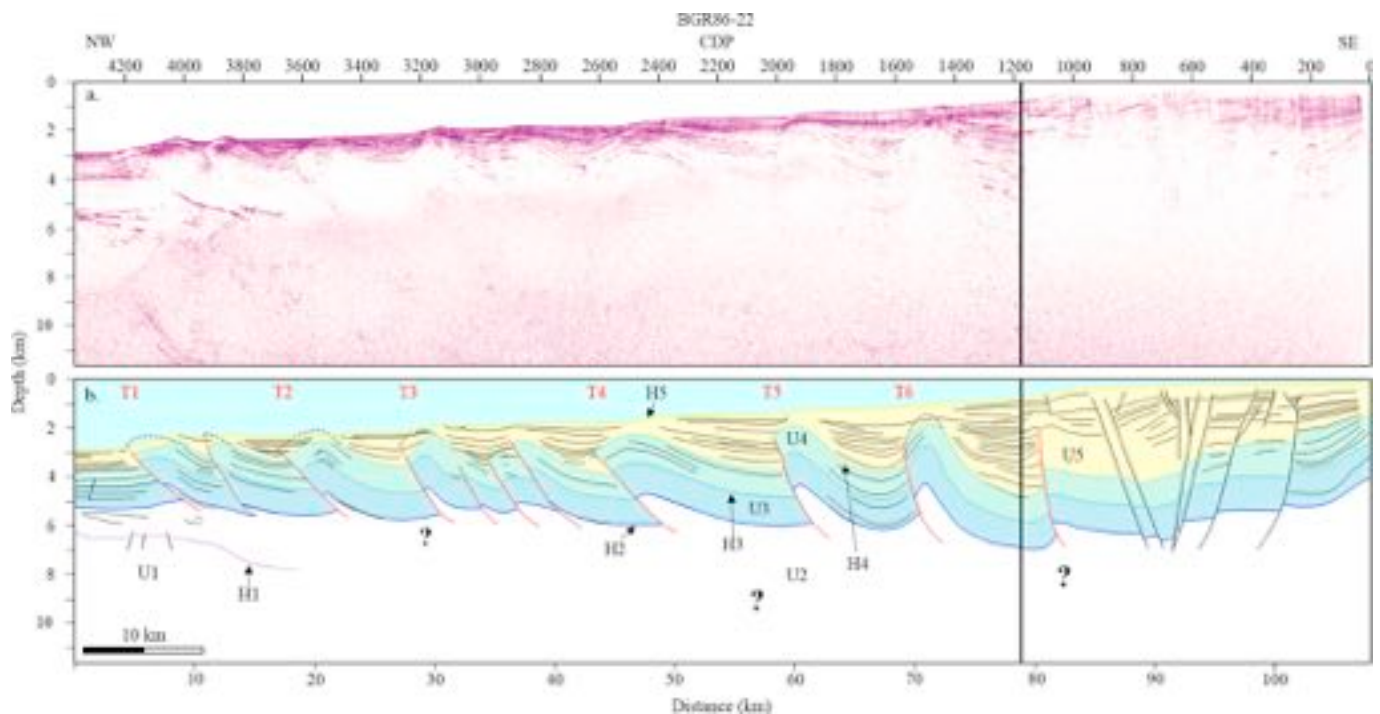
et al., 2008). It represents the top of the seismic unit U4, assigned as Early Pliocene by Hesse et al. (2009, 2010a, b). This unit is characterized by sub-parallel, continuous and medium to high-amplitude reflections. The attitude of reflections at the crests of the anticlines (Fig. 7b) suggests that substantial syn-tectonic erosion occurred during anticline growth.

Seismic horizon H5 represents the modern seafloor. H5 is of high amplitude and continuity. The underlying seismic unit U5 is Late Pliocene to recent in age (Hesse et al., 2009, 2010a; b), and characterized by continuous, medium to high frequency, high-amplitude reflections. Several reflections show wedge geometries indicating

strong syn-kinematic stratigraphic growth in active piggy-back basins (Fig. 7c). Onlap and downlap reflection geometries occur interbedded with chaotic seismic facies around deepwater anticlines; the chaotic facies zones can be interpreted as mass-transport accumulations (Fig. 7a,d). Inside individual piggy-back basins, seismic reflections tend to diverge toward the depocenter. In the upper part of U5, sub-horizontal and sub-parallel to parallel reflections occur. The seafloor is affected and deformed by folding and thrust propagation mainly in the frontal (seaward) part of the FTB.

Seismic lines BGR86-18 to BGR86-24 all display a similar structural style, characterized by a series of tectonic blocks separated by
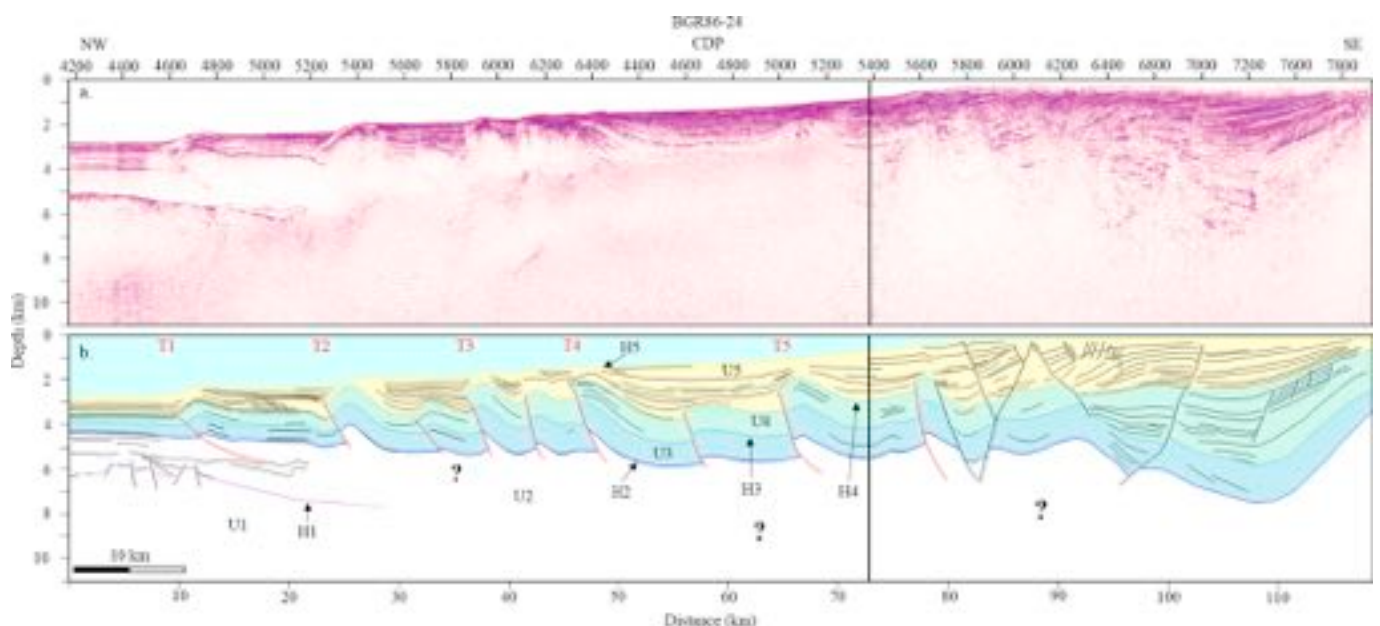

Fig. 6. (a) Uninterpreted seismic profile BGR86-24. (b) Initial interpretation of the seismic profile displaying the seismic units (U) and the seismic horizons (H). Names of the main thrust faults are labeled in red. Vertical exaggeration x2.
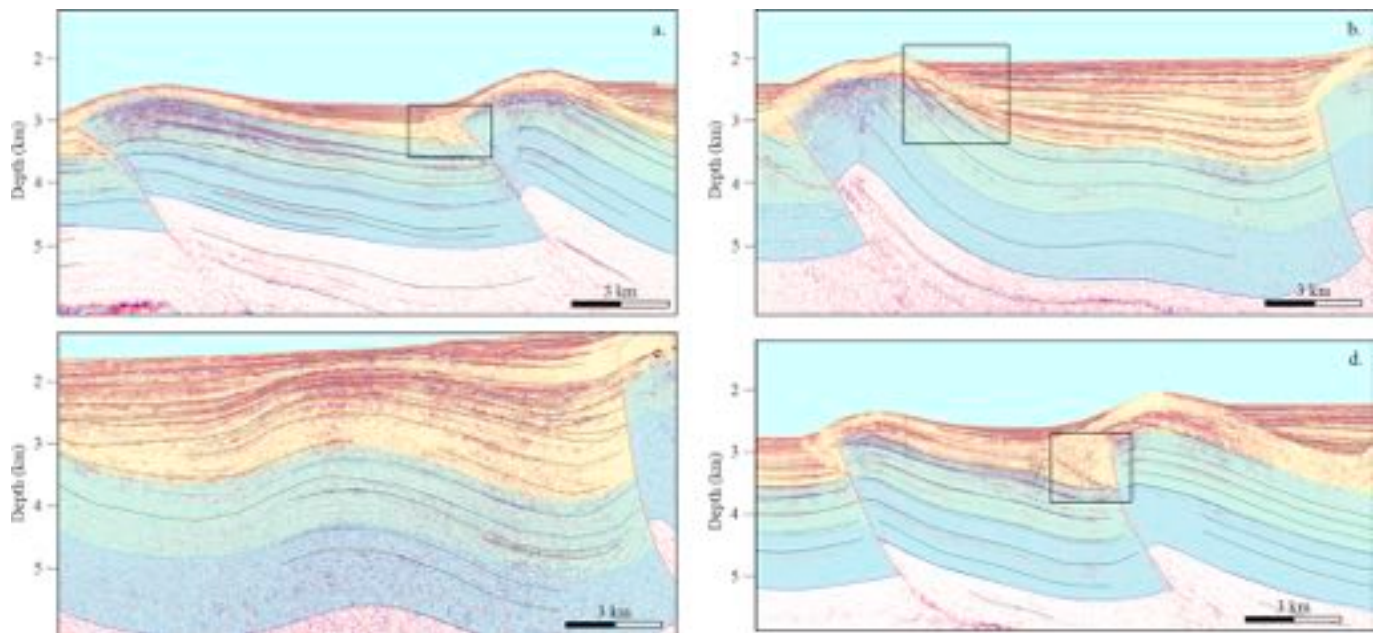
Fig. 7. Details of seismic profiles #18 (a, b, c) and #20 (d) showing: slumps and other mass-transport derived bodies, mainly developed within U5, in front of active thrusts (7a and 7d); onlap unconformities, testifying syntectonic deposition of U5, mainly evident at the back-limb of the anticlines (7a, 7b, 7c and 7d); strong erosion of top U4 at the anticlines crest (7a and 7b). Note that U2, U3 and U4 show only slight thickness variations, suggesting that most of the tectonic activity occurred after their deposition. Note also that shortening is still active, as evidenced by significant deformation/folding of the seafloor, especially in correspondence of the anticlines crests.

southeast-dipping thrust faults overlain by asymmetric, northwest-verging thrust-hangingwall anticlines. The acoustic basement is generally southeast-dipping; shelfal extensional faults and slope piggy-back basins occur on all lines, and the sedimentary succession generally thickens landward. However, the northern part of the study area (lines BGR86-18 and 20; Figs. 3 and 4) show some significant differences respect to the southern one (lines BGR86-22 and 24, Figs. 5 and 6). In the northern profiles, a ~70–80 km wide compressional domain dominates the sections and only few, minor extensional features occur in the most landward parts of the data. The main-thrust-related anticlines are widely spaced and strongly affect the seafloor. Shortening is accommodated by six main southeast-dipping thrust faults with few (two to three) minor splays (Figs. 3 and 4). In contrast, in the southern profiles, the compressional domain reduces to ~65–75 km in width (Figs. 5 and 6), and a ~20–30 km wide extensional domain characterizes the shelf and upper slope areas. The main-thrust-related anticlines are up to 11 km apart, showing a less pronounced surface expression. Shortening in this part of the FTB is accommodated by up to six main southeast-dipping thrust faults with several minor fault splays.

Considering all the four sections, the stratigraphic thickness of units U2 to U5 decreases northwestward (i.e. seaward) along dip (from ~5.7 km to ~2 km) and southwestward along strike (maximum thickness varies from ~5.7 km to ~5.4 km).

4. ADS method

4.1. Introduction

The Area-Depth-Strain (ADS) method can be used to balance geological cross-sections, quantify boundary fault displacement and folding, quantify uncertainties in the interpretation, locate detachments and infer the amount of subseismic strain from seismic profiles (Epard and Groshong, 1993; Groshong and Epard, 1994; Schlische et al., 2014; Groshong, 2015). The ADS method is an area-balance technique, which only assumes constant area without other limits (i.e. constant bed length and thickness during deformation; knowledge about mechanical properties of deformed units; kinematic evolution; e.g. Groshong,

2015). The method uses the depth of multiple regional levels and the excess area of each unit above these levels to plot an area-depth graph (Fig. 8; Epard and Groshong, 1993; Groshong and Epard, 1994; Groshong, 2015; Wang et al., 2017), therefore it is fully independent of length measurements and insensitive to bed-length variations (Epard and Groshong, 1993).

The original area-depth linear function in the area-depth plot is expressed by:

$$h = (1/D)S + H. \qquad (1)$$

where h is the distance from an arbitrary reference level to the regional level of the considered horizon, D is the boundary displacement (i.e. the horizontal shortening), S is the displaced area (or excess area) and H is the depth to detachment from the same arbitrary reference level at the Pin and Moving lines (Fig. 8). The sections to be balanced are comprised between two vertical boundary lines, named Pin Line and Moving Line, respectively; the Pin line represents a fixed point at the front of the compressional structures while the Moving line represents the inner, moving part of the compressional structures. The area-depth data of different stratigraphic horizons are interpolated by a straight line of which the inverse slope represents the boundary displacement and the intercept, at excess area = 0, is the depth to detachment (Epard and Groshong, 1993). The correlation coefficient R^2 represents how well the area-depth line fits the area-depth points (perfect fitting is $R^2 = 1$) and indicates if a geological section is balanced (Groshong et al., 2012; Wiltschko and Groshong, 2012; Schlische et al., 2014; Groshong, 2015; Wang et al., 2017). Eq. (1) was successfully applied to classic detachment folds (Epard and Groshong, 1993; Groshong and Epard, 1994; Gonzalez-Mieres and Suppe, 2006, 2011; Groshong, 2015), fault-propagation folds and ramp anticlines (Groshong, 2015), buckle-style detachment folds (Groshong, 2015) and fault-bend folds (Groshong et al., 2012; Wiltschko and Groshong, 2012; Schlische et al., 2014). Wang et al. (2017) modified eq. (1) to model the detachment of fold-thrust systems where layers become progressively thinner in one direction and where thrusting develops along a dipping, bed-parallel detachment.

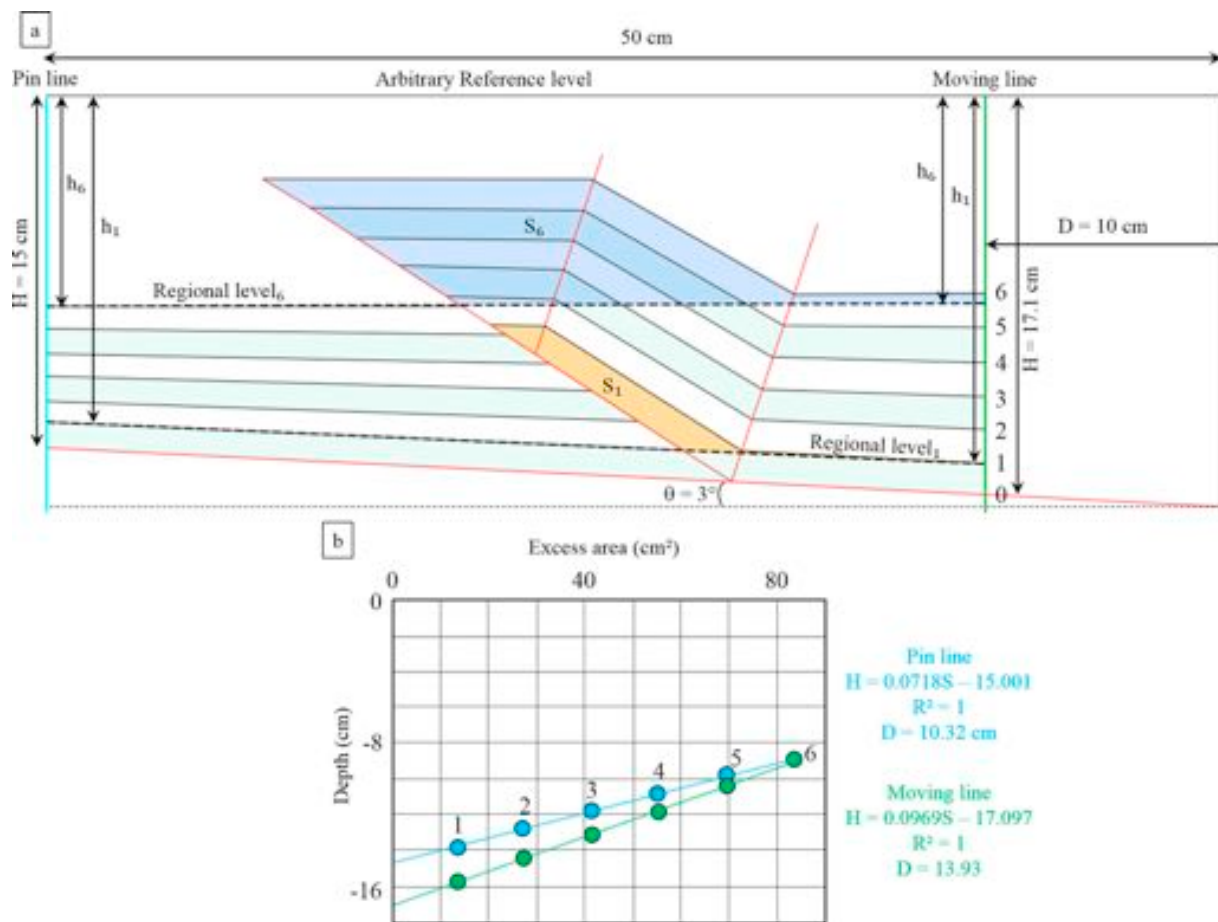The application of the ADS method requires caution when applied in

Fig. 8. Schematic section of the ADS method application. (a) Regional level, excess area (S) and depth of the regional level relative to the arbitrary reference level on the Pin and Moving lines for horizon 6 (in blue) and horizon 1 (in orange). (b) Area–depth graph. *h* is the distance from an arbitrary reference level to the regional level of the considered horizon; H is the obtained depth to detachment on the Pin and Moving lines; D is the boundary displacement (i.e. horizontal shortening). Modified after Wang et al. (2017).

structurally complex areas comprising duplexing, triangle zones, re-activation of precedent tectonics or break-thrusting, i.e. where older structures are not related to the major basal detachment of a younger fault formed in brittle stratigraphic intervals in correspondence of highly strained fold limbs (Morley et al., 2017). The presence of such complex structures may generate problems in determining the original regional level and the correct determination of the excess area, which may vary if affected by multiple deformation intervals. Another limitation of the ADS method is the requirement of i) at least two interpreted horizons and that ii) at least two of the interpreted horizons must be pre-growth horizons (for the area-depth line determination). This requirement might not be possible to meet in every fold-thrust system.

4.2. Application

Figs. 3–6 show that the geological information reflected by our seismic data strongly decreases in depths below 4–5 km. This makes the interpretation of the detachment level of the overlying thrust system ambiguous. Therefore, the ADS method by Wang et al. (2017) has been used to determine the detachment depth and dip, and to support improved balancing of the geological sections. Profile BGR86-22 is used as an example of the application of the ADS method (Fig. 9), and the same workflow and assumptions have been used for all seismic-geologic sections considered in this study (Fig. 10). The Pin line is located in undeformed reflections basin-ward of the NW Borneo FTB (see Fig. 2 for the Pin line position in map view). The Moving line is in correspondence with the axial surface of the innermost thrust-related syncline,

basin-ward of any extensional structure. The arbitrary reference level, necessary to calculate the depth of the horizon regional levels and of the detachment, is the sea level (e.g. Groshong, 2015) (Fig. 9). The three horizon regional levels are constructed by connecting the respective lowest points of each horizon at the axial surface of the synclines. This level is the best representation of an inferred pre-deformation position of the horizons H2, H3 and H4 (Fig. 9 c, d, e). The excess area of each unit (S_i) is bounded by the regional level at the base and by its top; the excess area decreases toward older units, thus $S_4 > S_3 > S_2$ (Fig. 9). The variability in depth between the Moving line and the Pin line as well as changes in dip of the horizon regional levels agree with an original wedge geometry, in which all units thicken toward the southeast (i.e. landward). Seismic horizon H4 forming the top of seismic unit U4 is partially eroded at the crests of fault-related anticlines. Schlische et al. (2014) performed a kinematic model and an analog model representative of a partially eroded thrust-ramp anticline, which demonstrated that, before erosion, pre-kinematic strata lay along the same area-depth line. Assuming that seismic units U2, U3 and U4 were deposited before they were deformed, or that they only underwent little syn-depositional shortening, their area-depth data should fit the same straight line. The area-depth data of H4, after the reconstruction of the eroded parts, is well aligned with the area-depth line interpolating H2 and H3 therefore the reconstruction is plausible on all seismic sections (Fig. 10). Moreover, the obtained high correlation coefficient (R^2) shows that the sections are quantitatively balanced (Groshong, 2015). All previously interpreted thrust faults were finally extrapolated in depth and linked to the ADS-defined detachment level assuming a
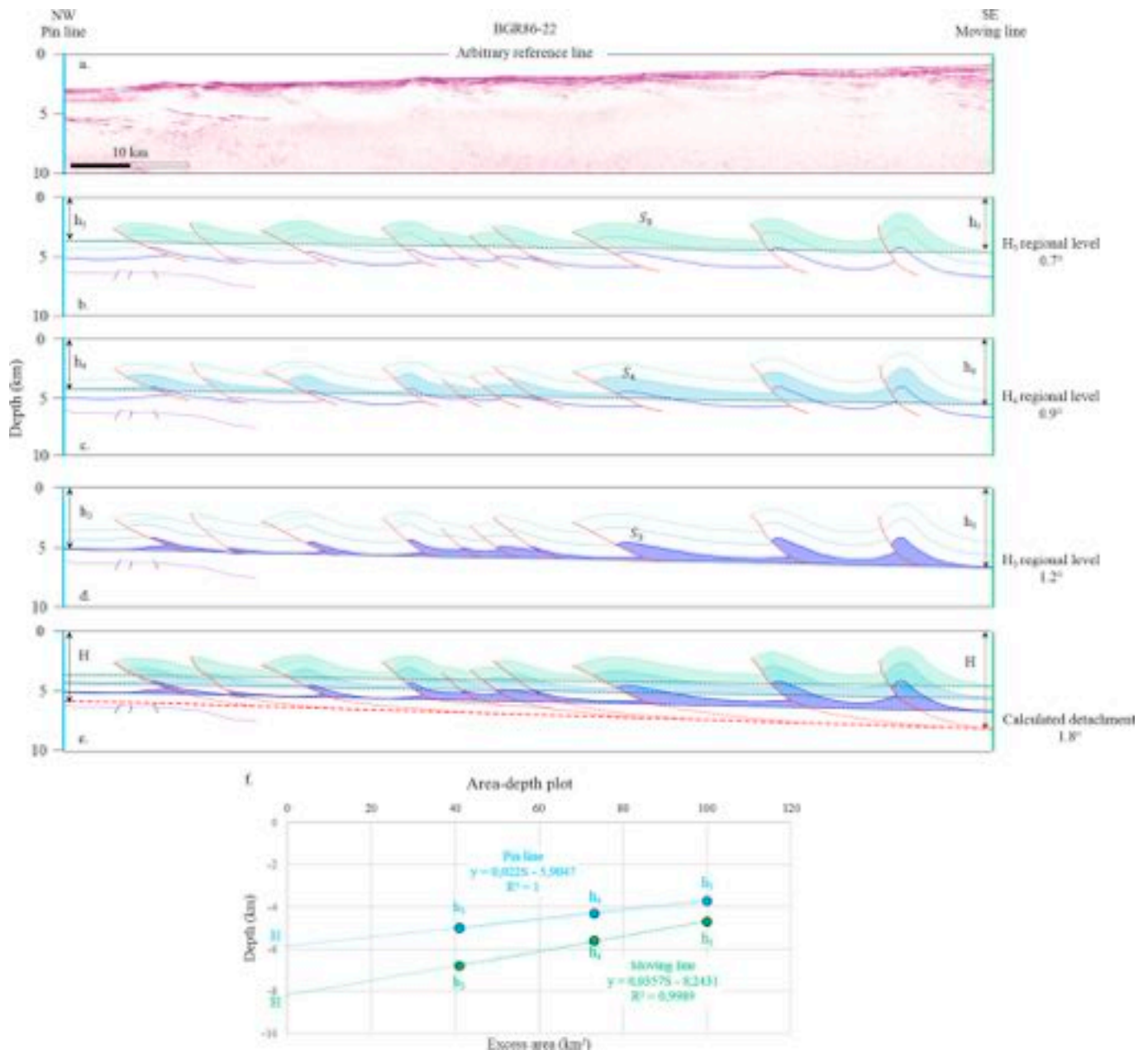
Fig. 9. ADS method workflow for the seismic profile BGR86-22. (a) Seismic profile. (b) Regional level and excess area (S$_5$) for horizon H5. (c) Regional level and excess area (S$_4$) for horizon H4. (d) Regional level and excess area (S$_3$) for horizon H3. (e) Depth of the detachment (black dashed line)obtained from the ADS method. (f) Area-depth graph showing the results of the ADS method. Si is the excess area, hi is the depth of the regional level relative to the reference level on the pin and moving lines, H is the depth of the detachment relative to the reference level on the pin and moving line.

slightly listric geometry, particularly keeping account for the geometry of the respective thrust-hangingwall folds (Fig. 10).

The application of the ADS method ultimately allows to reconstruct a landward-dipping (i.e. ESE) detachment level with an average dip of 1.9° (Table 1), whose depth generally decreases southward, being ~ 5.6 km at the Pin line to ~ 8.7 km at the Moving line to the north and ~ 4.9 km at the Pin line to ~ 7.3 km at the Moving line to the south (Fig. 10).

4.3. Calibration of results

We tested the plausibility of the detachment depth and attitude, derived by the application of the ADS method, following two different approaches.

Firstly, we compared our results with the reconstruction proposed by Franke et al. (2008), who traced on seismic line BGR01-10 a shallow, strong, slightly southeast-dipping reflection, interpreted as the main basal detachment of the NW Borneo FTB. Seismic line BGR01-10 is, however, oriented N160° and intersects, with an angle of ~ 44°, three of the seismic profiles interpreted in this study (BGR86-18, BGR86-20 and BGR86-22). The obliqueness of line BGR01-10 to the main structural elements (Fig. 2) suggests that the dip angle of the displayed detachment is only apparent. However, the depth of the detachment at the respective intersections with lines BGR86-18 and BGR86-20 represents its actual position. The intersections could be therefore used to calibrate the ADS-determined depth of detachment on these seismic lines. The intersection along line BGR86-22 is located within the extensional domain and was therefore not considered. The differences in depth
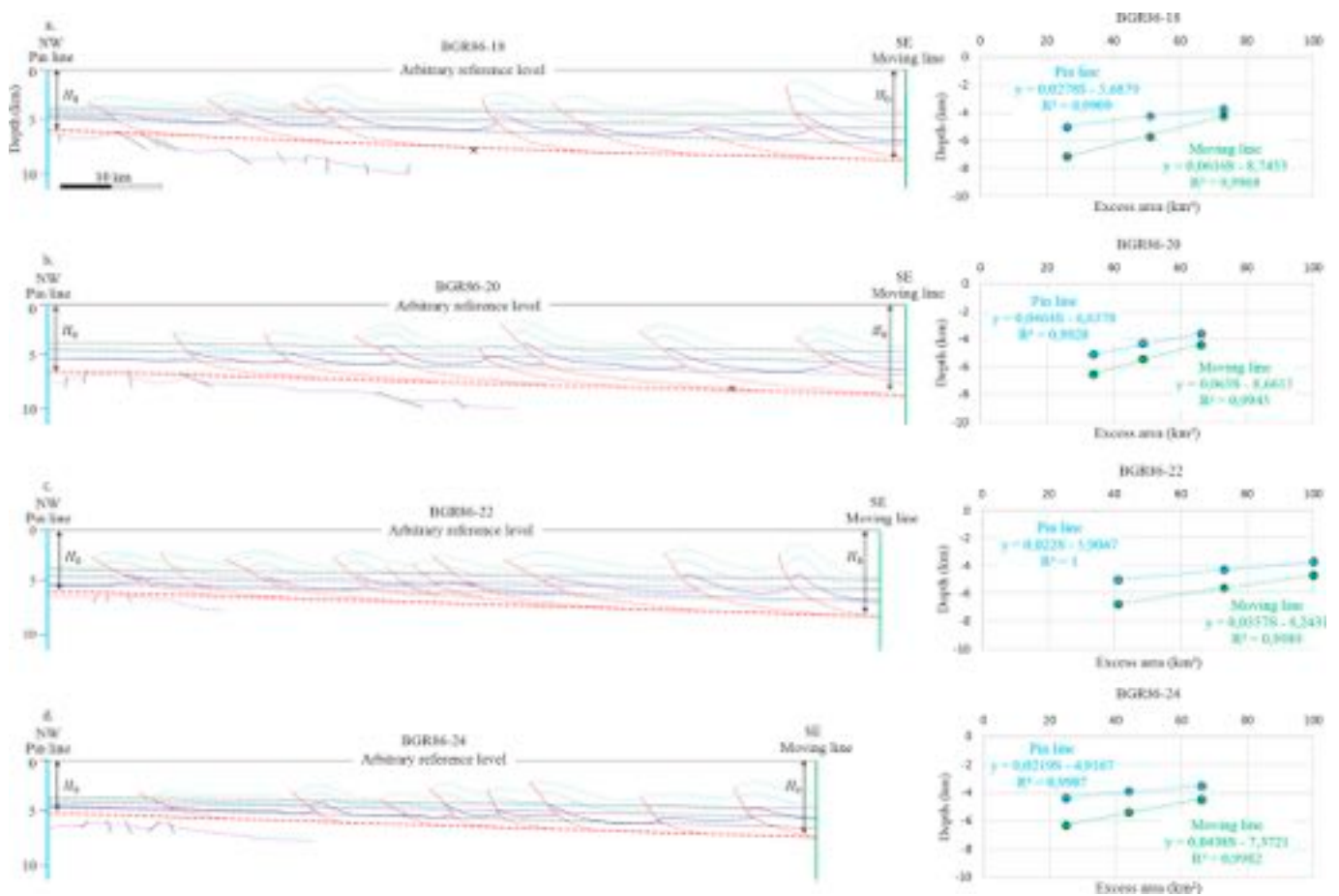
Fig. 10. Results of the ADS method applied to all seismic profiles. Red dotted lines are the determined basal detachment. Black crosses in (a.) and (b.) represent the intersection points between the detachment displayed by Franke et al. (2008) and the seismic profiles used in this work.

Table 1
Values of alpha and beta along each section.

Seismic profile	α	β	α + β
86–18	1.5°	2°	3.5°
86–20	1.5°	1.9°	3.4°
86–22	1.5°	1.8°	3.3°
86–24	1.5°	1.9°	3.4°

Fig. 11. Fold wavelength vs. stratigraphic thickness of the central part of the NW Borneo FTB (N Baram FTB) compared with 9 shale-detached DWFTB from Morley et al., (2011) (modified after Cruciani et al., 2017).

between the ADS-determined detachment and the intersections at line BGR01-10 are $\Delta z = \sim 400$ m at BGR86-18 and $\Delta z = \sim 180$ m at BGR86-20 (Fig. 10a and b); these differences represent a 5% and a 2.5% error, respectively, which can be considered a reasonable agreement (Groshong, 2015). A similar qualitative detachment prediction to that of Franke et al. (2008) based on different industry seismic-reflection data is provided by Cullen (2010; his Figs. 8–10, 12) who also mapped a slightly south-east dipping detachment (depth between 4.5 and 7 s TWT).

Another second test of the plausibility of the ADS detachment prediction was obtained by plotting stratigraphic thickness and fold wavelength sensu Morley et al. (2011). The plot on Fig. 11 shows that deformed stratigraphic thickness considered in this work and the fold wavelength values are in agreement with the positive correlations obtained for other fold-and-thrust belts developed in deepwater environment (deepwater fold-and-thrust belts; DWFTBs) case studies, detached on shales.
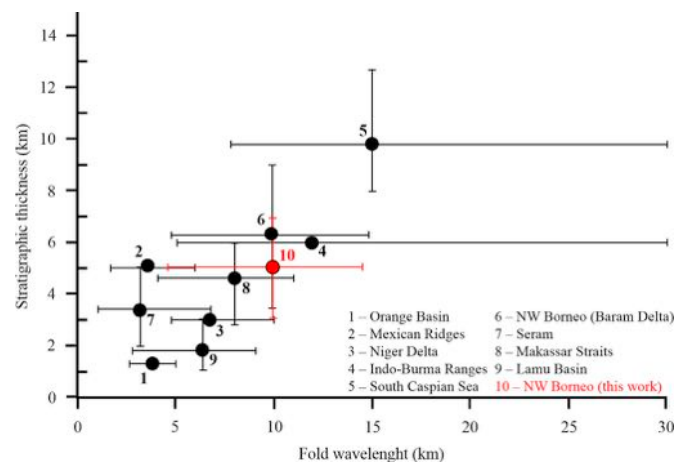
5. Discussion

In order to discuss the implications of the ADS approach of this study, in comparison with previous tectonic reconstructions of the NW Borneo FTB, a series of 2D sequential restoration was performed along seismic lines BGR86-18, BGR86-20, BGR86-22 and BGR86-24. The 2D restoration procedure was identical along each profile, consisting of three subsequent steps (Fig. 12): i) back-stripping including the
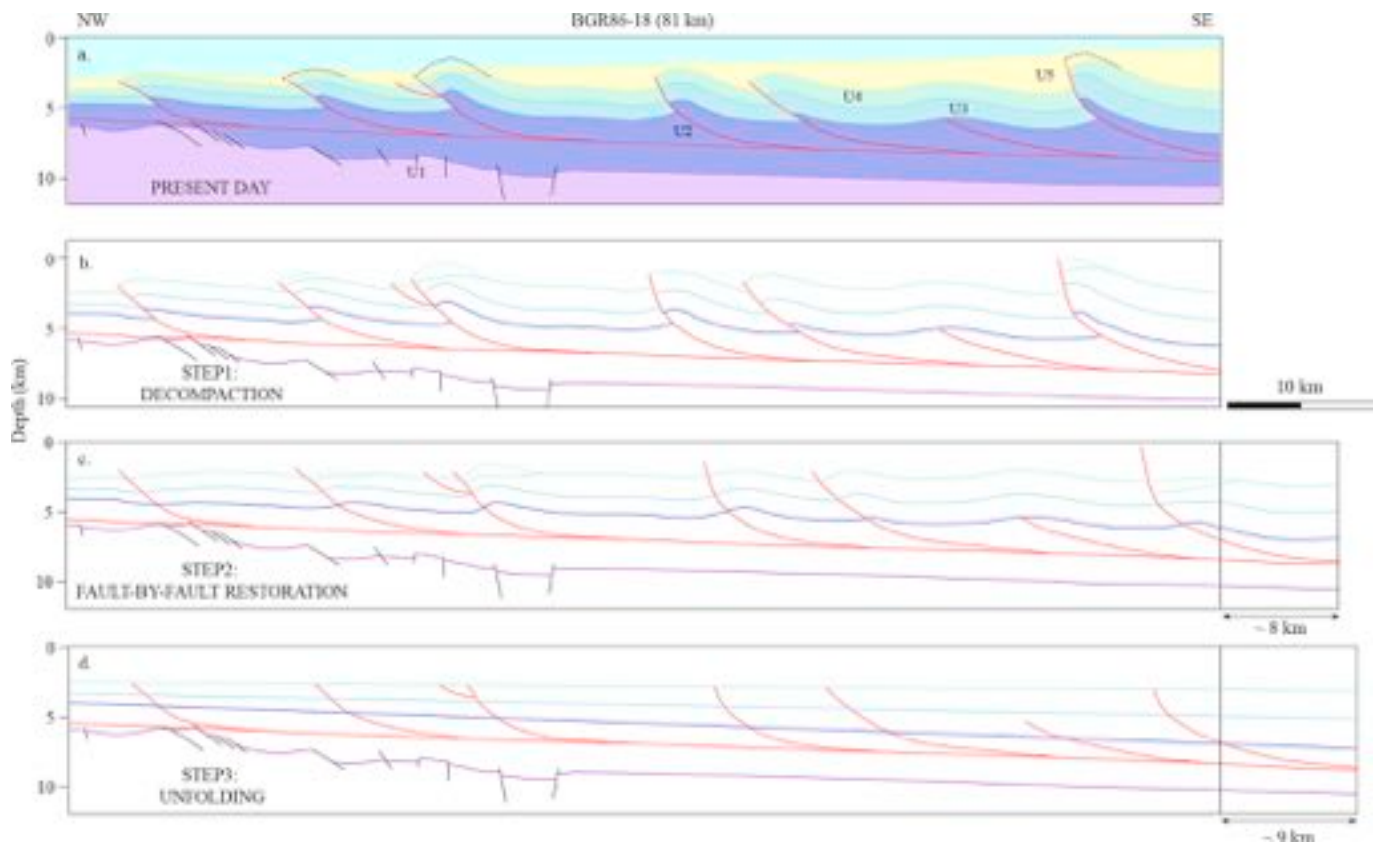
Fig. 12. Representative example of the tectonic restoration workflow (seismic profile BGR86-18) performed at the outer compressional part of the central part of the NW Borneo FTB. (a.) The 81 km long section displays the present day geological situation; the black dotted lines represent the eroded areas of U5. (b.) The interpreted section after decompaction of the Pliocene to recent piggy-back basin deposits; the thickness of the pre-kinematics units increases of ~1 km. (c.) Section after complete fault restoration; the amount of shortening due to thrusting is ~8 km. (d.) Section after the unfolding of each horizon; the shortening due to folding is ~1 km.

decompaction of syn-kinematic deposits (*sensu* Sclater and Christie, 1980), followed by an isostatic correction (*sensu* Burov and Diament, 1992); ii) fault-by-fault retro-deformation (fault parallel flow algorithm *sensu* Egan et al., 1997); and iii) fold-by-fold unfolding (flexural slip algorithm *sensu* Griffiths et al., 2002). The fault-by-fault and fold-by-fold retro-deformation steps were carried out assuming a general in-sequence thrust propagation, starting from the restoration of the displacement along the frontal thrust fault, moving landward. Shortening associated to thrusting and folding was measured incrementally along fixed lines, located at the undeformed parts of each main thrust sheet (generally corresponding to almost flat strata at the synclines core) to record the total bulk shortening (Fig. 13).

The measured total amount of shortening varies across the study area between ~6 km and ~14 km. The highest values are measured across the central lines BGR86-20 and BGR86-22 with ~12 km (13%) and ~14 km (15%) respectively and decrease toward the north and south (lines BGR86-18 and BGR86-24; ~9 km (10%) and ~6 km (8%) respectively; see Fig. 13). The contribution of the net slip along thrusts generally accounts for ~90% of the total shortening, while the thrust-associated folding generally accounts only for ~10%.

Cumulative shortening increases almost linearly along dip (Fig. 13). However, analyzing the deformation along each thrust fault, most of the shortening is accommodated by the central part of the FTB, decreasing landwards and basinwards. This suggests that the present deformation is active not only at the frontal thrust, which is the latest developing structure and it is still accumulating shortening, but also at the central thrust faults, besides they already have accommodated most of the shortening; the innermost thrust faults, instead, are presently inactive. The lower amount of total shortening accommodated by the

innermost thrust faults may be related to the larger amount of syn-tectonic deposits, which contributed to a major wedge thickening in this sector. An analysis of the syn-kinematic sedimentation patterns and seafloor features also allows to determine which parts of the DWFTB are still active (sensu Morley, 2009). The interpretation of the seismic data (Figs. 3–6) shows that the seafloor is deformed only in the central and frontal parts of the FTB. The larger thickness variations between the piggy back-basin depocenters and the top anticlines are observed within unit U5, suggesting that most of the shortening occurred starting from ~3.6 Ma. This interpretation indicates an average Late Pliocene to recent shortening rate in the offshore southern Sabah study area of ~3 mm/yr, a value that is consistent with the present day short-term convergence rate obtained by GPS data by Sapin et al. (2013) but differs significantly from other GPS-derived shortening interpretations made by e.g. Rangin et al. (1999) and Simons et al. (2007) who measured larger values of convergence. Morley (2009) in turn, by studying the growth of folds offshore Brunei suggested an average shortening rate of around 2 mm/yr for the last ~3 Ma. He considered this shortening rate, if strain partitioning occurred, as an underestimation due to the obliquity of the differential motion between south Borneo and NW Borneo (~3–4 mm/yr), which occurs at ~45° to the orientation of the main fold systems.

The results of the ADS analysis forwarded in this paper can be furthermore discussed against the critical taper theory (Davis et al., 1983; Dahlen, 1990). According to this theory, the overall FTB wedge geometry is described by the angle α + β, where α and β are the slope of the top surface and the dip of base of the wedge, respectively. The higher α and β, the shorter and thicker is the wedge. The wedge geometry is controlled by several factors, including: i) pore pressure within
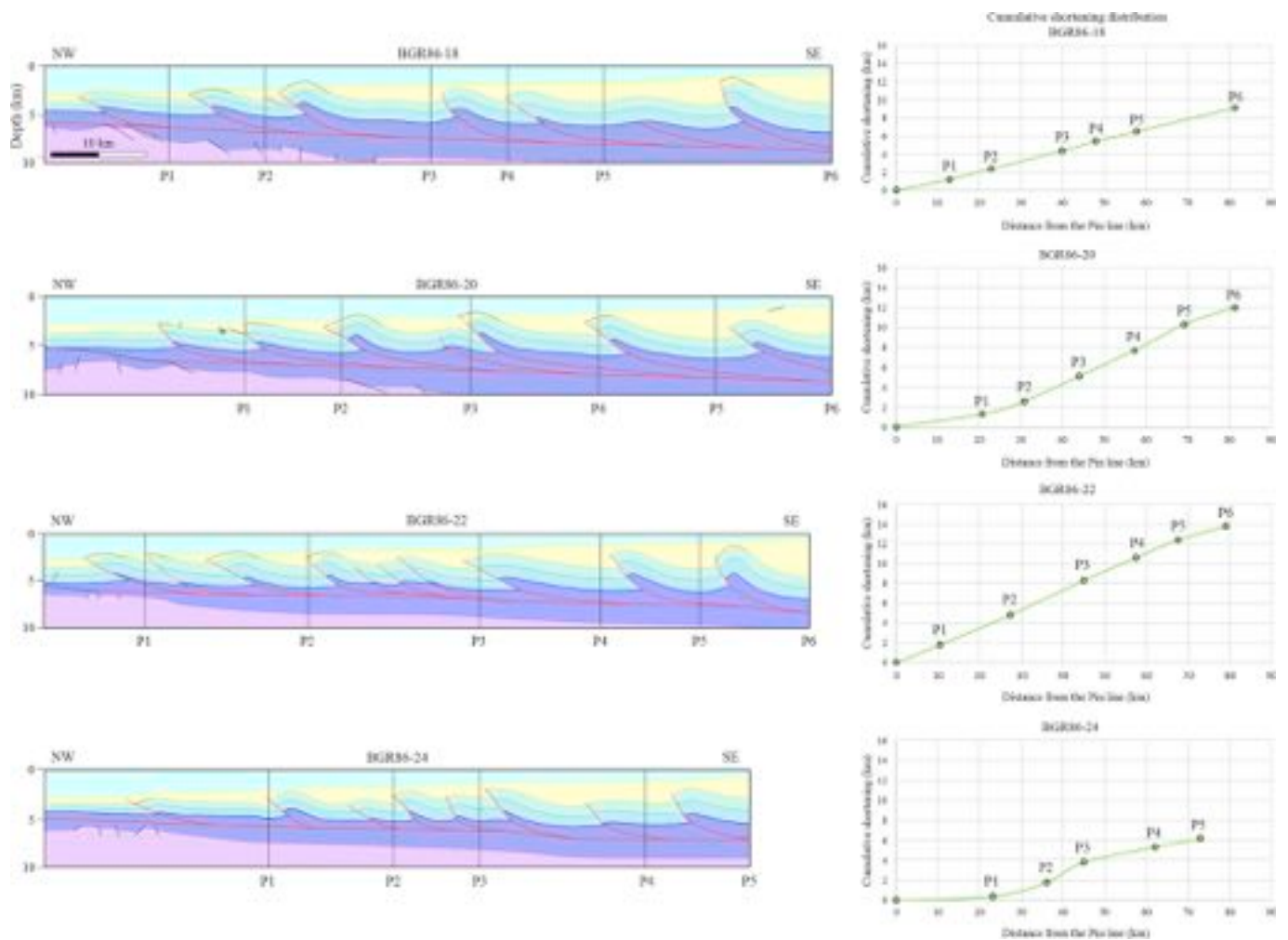
Fig. 13. Shortening distribution along each seismic profile. The interpolation line which connect the pin lines along each section is oriented parallel to the general strike of the thrust faults (black dashed line in Fig. 2b).

the wedge and at its base, ii) wedge strength and iii) detachment strength. Detachment strength is, in turn, directly affected by the rheology of the accreted material, the differential load induced by along-strike thickness variations, the friction coefficient at the base of the wedge, dip and dip direction of α and β, overpressure (King and Morley, 2017, and references therein) and the pervasive foliation of the fault rocks (Tesei et al., 2015). The ADS method permits measurement of the wedge-taper angle with high accuracy and provides constraints for the mechanical evolution of the NW Borneo FTB. The measured dip of the top surface (α) is ~1.5° (Table 1). The dip of the base of the wedge (β) varies between 2° and 1.8° (Table 1; average β = 1.9°). α and β determine an average wedge-taper angle of 3.4°, values that are significantly lower than previous estimations (e.g. Hesse et al., 2009) where e.g. β alone was considered to have a maximum of 6°, and an average of 3.5°.

Morley (2007) suggests that these low values of α and β angles in this area can be related to high pressure (near lithostatic pressure: $\lambda_b \sim 1$) within the basal detachment. However, according to Tesei et al. (2015), if a low friction of foliated fault rocks is taken in account, a slightly lower fluid pressure is required, which should not exceed $\lambda_b \sim 0.8$. The relatively low taper angle value, the flat geometry of the foredeep basin and the stepped slope profile of the FTB yet contrast with the typical geometries of sediment-supply dominated continental margins, and suggest that the NW Borneo FTB is at, or close to, critical taper, thus actively growing basinwards (Morley, 2007).

Fig. 14 shows the ADS-calculated values of the central part of the

NW Borneo FTB wedge-taper angle (α = 1.5° and β = 1.9°) in a wedge strength (W) vs. fault strength (F) diagram sensu Suppe (2007), modified by King and Morley (2017). The modification made by the latter authors, re-arranged the original critical-taper equations (Davis et al., 1983; Dahlen, 1990), constraining all possible values for W and F solely based on the wedge-taper angle measurement, excluding the pore pressure and the friction coefficient. The W and F values calculated for NW Borneo fall between the near-field stress-driven and the mixed near- and far-field stress DWFTBs, close to two DWFTB case studies, driven by far-field stress and characterized by high sedimentation rate (e.g. Makran and Barbados accretionary prisms, see King and Morley, 2017). However, based on its geological history, the wedge-taper angle ranges suggested by King and Morley (2017) and from the Plot of Wedge Strength vs. Fault Strength (Suppe, 2007; King and Morley, 2017) this portion of the NW Borneo deepwater fold-and-thrust belt, can be better interpreted as a mixed near- and far-field stress-driven DWFTB.

6. Conclusions

The ADS method was successfully applied to the central part of the NW Borneo FTB, helping to estimate a reliable depth and geometry of the basal detachment. The method was applied to four geological sections, derived from the interpretations of a set of seismic reflection profiles, where the detachment was not clearly imaged. Our results show that in the study area the detachment dips about 1.9° towards ESE
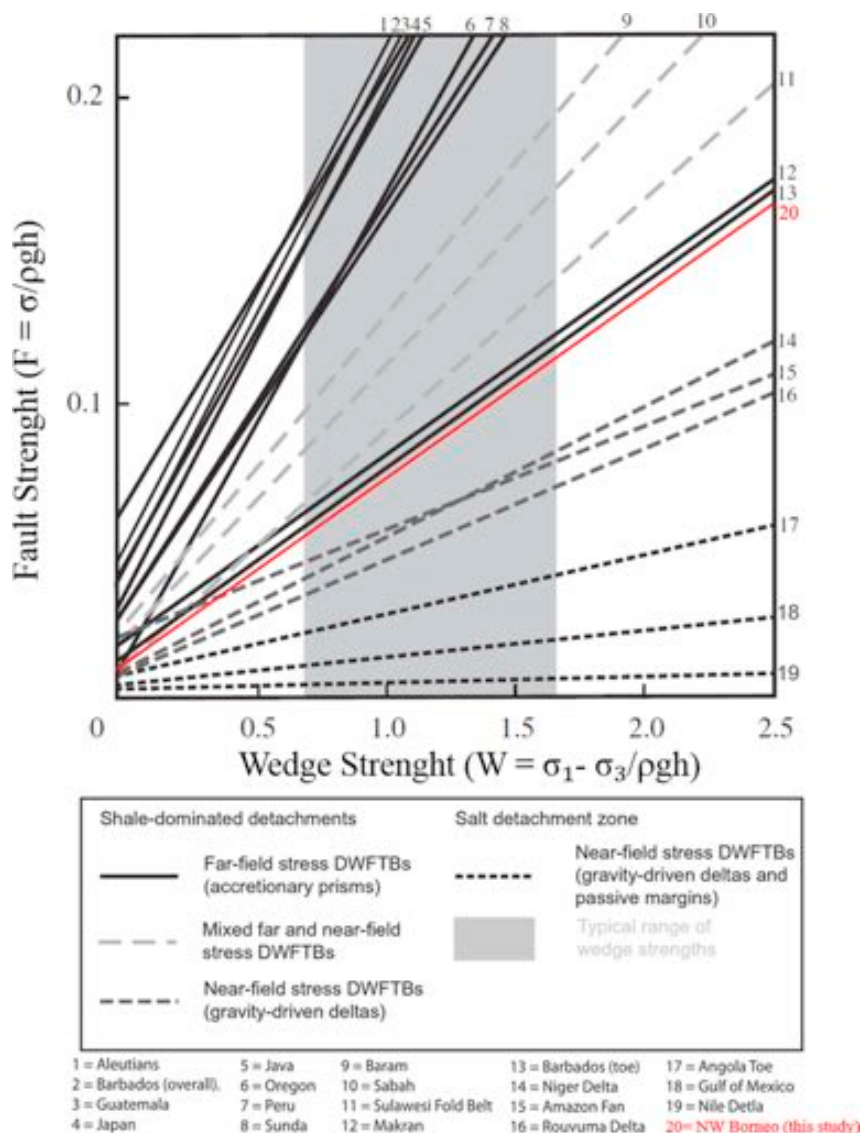
Fig. 14. Plot from King and Morley (2017). The Fault Strength-Wedge Strength straight line falls between near-field stress and mixed far and near-field stress DWFTBs.

(i.e. landward) and it is located at depth which generally decreases southward being 5.6 km at the Pin line to 8.7 km at the Moving line to the north and 4.9 km at the Pin line to 7.3 km at the Moving line to the south.

The obtained depth is coherent with the observations collected along a more recent seismic profile (BGR01-10 from Franke et al., 2008), imaging the detachment; however, since the profile is oblique respect to the detachment dip, it does not represent its true dip, and has been used to verify the detachment depth at the intersection points with the profiles interpreted in this study. The obtained depth to detachment is also consistent with the detachment suggested by Cullen (2010). A further test of the results, based on the correlation between fold wavelength and stratigraphic thickness, also showed that the ADS-calculated detachment provided an improved kinematic reconstruction of the FTB along the four considered sections.

Using the ADS-based detachment geometry, we performed a new restoration procedure, furnishing new, possibly more realistic values of shortening and shortening rate. The ADS method also allowed to check the reliability of reconstruct eroded areas of pre-kinematics beds and enabled the analysis of the NW Borneo FTB with respect to the critical wedge theory.

The wedge taper angle measured using the dip of the basal detachment (β) determined by the use of the ADS method is representative of a mixed near- and far-field stress DWFTB, affected by crustal shortening with a gravity component. Seismic interpretation and kinematic reconstruction indicated that most of the shortening occurred mainly in the last ~3.6 Ma, and that, folding and faulting are still active in both the central and outer part of the thrust belt. The total amount of shortening tends to increase towards the central part of the system, consequently the shortening rate varies, being maximum at the center (~3 mm/yr at BGR86-20, to ~ 4 mm/yr at BGR86-22) decreasing towards the edges (~3 mm/yr at BGR86-18, to ~ 2 mm/yr at BGR86-24). For this part of the fold-and-thrust belt an average shortening rate of ~3 mm/yr was then calculated for the past 3.6 Ma.

In summary, the ADS method proves valuable, particularly in settings where subsurface knowledge of the basal detachment level is limited or debated, which is a common case in many different tectonic environments worldwide, in both off-shore and on-shore FTBs. Where thrust belt is sub-aerial, there are often very detailed reconstructions of the structures mapped at the surface; on the contrary, the seismic quality is often poor, and hampers a well constrained reconstruction of the depth and geometry of the basal detachment. Typical cases are the

Apennines of Italy (e.g. Massoli et al., 2006; Barchi, 2010) and the Eastern Cordillera of the Andes (e.g. Allmendinger et al., 1990; Kley et al., 1999). Also in offshore areas, as in the case illustrated in this paper, the basal detachment may be difficult to be definitely recognized, mainly because of quality/resolution decrease of seismic data at depth. In all these settings, a thoughtful application of the ADS method is recommended, to help better constrain the fundamental base of FTBs.

Declarations of interest

None.

Acknowledgements

References

Allmendinger, R.W., Figueroa, D., Snyder, D., Beer, J., Mpodozis, C., Isacks, B.L., 1990. Foreland shortening and crustal balancing in the Andes at 30°S latitude. Tectonics 9, 789–809.

Barchi, M.R., 2010. The Neogene-Quaternary evolution of the Northern Apennines: crustal structure, style of deformation and seismicity. In: Marco Beltrando, Angelo Peccerillo, Massimo Mattei, Sandro Conticelli, and Carlo Doglioni, Journal of the Virtual Explorer, vol. 36. pp. 10.

Barckhausen, U., Roeser, H.A., 2004. Seafloor spreading anomalies in the SCS revisited. In: In: Clift, P., Wang, P., Kuhnt, W., Hayes, D. (Eds.), Continent-ocean Interactions within East Asian Marginal Seas. Geophysical Monograph, vol. 149. AGU, Washington, D,C, pp. 121–126.

Briais, A., Patriat, P., Trapponier, P., 1993. Updated interpretation of magnetic anomalies and seafloor spreading stages in the South China Sea: implications for the Tertiary tectonics of Southeast Asia. J. Geophys. Res. 98, 6299–6328.

Burov, E.B., Diament, M., 1992. Flexure if the continental lithosphere with multilayered rheology. Geophys. J. Int. 19, 617–620.

Chamberlin, R., 1910. The Appalachian folds of central Pennsylvania. J. Geol. 228–251.

Cruciani, F., Barchi, M.R., Koyi, H.A., Porreca, M., 2017. Kinematic evolution of a regional-scale gravity-driven deepwater fold-and-thrust belt: The Lamu Basin case-history (East Africa). Tectonophysics 712–713, 30–44.

Cullen, A.B., 2010. Transverse segmentation of the Baram-Balabac Basin, NW Borneo: refining the model of Borneo's tectonic evolution. Petrol. Geosci. 16, 3–29.

Davis, D., Suppe, J., Dahlen, F.A., 1983. Mechanics of fold-and-thrust belts and accretionary wedges. J. Geophys. Res. 88, 1153–1172.

Dahlen, F., 1990. Critical taper model of fold-and-thrust belts and accretionary wedges. Annu. Rev. Earth Planet Sci. 18, 55–99.

Egan, S.S., Buddin, T.S., Kane, S.J., Williams, G.D., 1997. Three-dimensional modelling and visualisation in structural geology: new techniques for the restoration and balancing of volumes. Proceedings of the 1996 geoscience information group conference on geological visualisation. Electron Geol. 1, 67–82.

Eichelberger, N.W., Nunns, A.G., Groshong Jr., R.H., Hughes, A.N., 2017. Direct estimation of fault trajectory from structural relief. AAPG Bull. 101, 635–653.

Epard, J.L., Groshong Jr., R.H., 1993. Excess area and depth to detachment. AAPG Bull. 77, 1291–1302.

Franke, D., Barckhausen, U., Heyde, I., Tingay, M.R.P., Ramli, N., 2008. Seismic images of a collision zone offshore NW Sabah/Borneo. Mar. Petrol. Geol. 25, 606–624.

Gonzalez-Mieres, R., Suppe, J., 2006. Relief and shortening in detachment folds. J. Struct. Geol. 28, 1785–1807.

Gonzalez-Mieres, R., Suppe, J., 2011. Shortening histories in active detachment folds based on area-of-relief methods. In: In: McClay, K., Shaw, J., Suppe, J. (Eds.), Thrust-fault Related Folding Vol. 4. AAPG Memoir, pp. 39–67.

Griffiths, P., Jones, S., Salter, N., Schaefer, F., Osfield, R., Reiser, H., 2002. A new technique for 3-D flexural slip restoration. J. Struct. Geol. 24, 787–814.

Groshong Jr., R.H., 1994. Area balance, depth to detachment, and strain in extension. Tectonics 13, 1488–1497.

Groshong Jr., R.H., 2015. Quality control and risk assessment of seismic profiles using area-depth-strain analysis. Interpretation 3 SAA1-SAA15.

Groshong Jr., R.H., Epard, J.-L., 1994. The role of strain in area-constant detachment folding. J. Struct. Geol. 16, 613–618.

Groshong Jr., R.H., Withjack, M.O., Schlische, R.W., Hidayah, T.N., 2012. Bed length does not remain constant during deformation: recognition and why it matters. J. Struct. Geol. 41, 86–97.

Hall, R., 1996. Cenozoic SE Asia. In: In: Hall, R., Blundell, D.J. (Eds.), Tectonic Evolution of SE Asia, vol. 106. Geological Society (London) Special Publication, pp. 153–184.

Hall, R., 2002. Cenozoic geological and plate tectonic evolution of SE Asia and the SW pacific: computed-based reconstructions, model and animations. J. Asian Earth Sci. 20, 353–431.

Hall, R., 2013. Contraction and extension in northern Borneo driven by subduction rollback. J. Asian Earth Sci. 76, 399–411.

Hall, R., Van Hattum, M.W., Spakman, W., 2008. Impact of India-Asia collision on SE Asia: the record in Borneo. Tectonophysics 451, 366–389.

Hamilton, W., 1979. Tectonics of the Indonesian Region. pp. 1–345 USGS Professional paper 1.078.

Hazebroek, H.P., Tan, D.N.K., 1993. Tertiary tectonics evolution of the NW Sabah continental margin. In: In: Geh, G.H. (Ed.), Proceedings of the Symposium on Tectonic Framework and Energy Resources of the Western Margin of Pacific Basin, vol. 33. Geological Society of Malaysia Bulletin, pp. 195–210.

Hesse, S., Back, S., Franke, D., 2009. The deep-water fold-and-thrust belt offshore NW Borneo: gravity-driven versus basement-driven shortening. Geol. Soc. Am. Bull. 121, 939–953.

Hesse, S., Back, S., Franke, D., 2010a. Deepwater folding and thrusting offshore NW Borneo, SE Asia. Geol. Soc. Spec. Publ. 348, 169–185.

Hesse, S., Back, S., Franke, D., 2010b. The structural evolution of folds in a deepwater fold and thrust belt – a case study from the Sabah continental margin offshore NW Borneo, SE Asia. Mar. Petrol. Geol. 27, 442–454.

Hinz, K., Schlüter, H.U., 1985. Geology of the dangerous grounds, South China Sea and the continental margin off Southwest Palawan: results of SONNE cruises SO-23 and SO-27. Energy 10, 297–315.

Hinz, K., Fritsch, J., Kempter, E.H., Manaaf Mohammad, A., Meyer, H., Mohamed, D., Vosberg, H., Weber, J., Benavides, J.J., 1989. Thrust tectonics along the continental margin of Sabah, northwest Borneo. Geol. Rundschau 78, 705–730.

Holloway, N.H., 1981. North palawan block, Philippines: its relation to Asian mainland and role in evolution of south China sea. Am. Assoc. Petrol. Geol. Bull. 66, 1355–1383.

Hubert-Ferrari, A., Suppe, J., Wang, X., Jia, C., 2005. Yakeng detachment fold, south Tianshan, China. Seismic interpretation of contractional fault-related folds. AAPG Seismic Atlas 110–113.

Hutchison, C.S., 1996. The 'Rajang accretionary prism' and 'Lupar Line' problem of Borneo. In: In: Hall, R., Blundell, D. (Eds.), Tectonic Evolution of Southeast Asia 106. Geol. Soc. of London Special Publication, pp. 247–261.

Hutchison, C.S., 2004. Marginal basin evolution: the southern South China Sea. Mar. Petrol. Geol. 21 (9), 1129–1148.

Ingram, G.M., Chisholm, T.J., Grant, C.J., Heldlund, C.A., Stuart-Smith, P., Teasdale, J., 2004. Deepwater North West Borneo: hydrocarbon accumulation in an active fold and thrust belt. Mar. Petrol. Geol. 21, 879–887.

James, D.M.D., 1984. Regional geological setting. In: James, D.M.D. (Ed.), The Geology and Hydrocarbon Resources of Negara Brunei Darussalam: Bander Seri Begawan, Brunei Darussalam. Brunei Museum and Brunei Shell Petroleum Company, pp. 34–42.

King, R.C., Tingay, M.R.P., Hillis, R.R., Morley, C.K., Clark, J., 2009. Present-day stress orientations and tectonic provinces of the NW Borneo collisional margin. J. Geophys. Res. 115, B10415.

King, R.C., Backé, G., Morley, C.K., Hillis, R.R., Tingay, M.R.P., 2010a. Balancing deformation in NW Borneo: quantifying plate-scale vs. gravitational tectonics in a delta and deepwater fold-thrust belt system. Mar. Petrol. Geol. 27, 238–246.

King, R.C., Tingay, M.R.P., Hillis, R.R., Morley, C.K., Clark, J., 2010b. Present-day stress orientation and tectonic provinces of the NW Borneo collisional margin. J. Geophys. Res. 115, B10415.

King, R.C., Morley, C.K., 2017. Wedge geometry and detachment strength in deepwater fold-thrust belts. Earth Sci. Rev. 165, 268–279.

Kley, J., Monaldi, C.R., Salfity, J.A., 1999. Along-strike segmentation of the Andean foreland: causes and consequences. Tectonophysics 301, 75–94.

Levell, B.K., 1987. The nature and significance of regional unconformities in the hydrocarbon bearing Neogene sequence offshore West Sabah. Geol. Soc. Malays. Bull. 21, 55–90.

Massoli, D., Koyi, H.A., Barchi, M.R., 2006. Structural evolution of a fold and thrust belt generated by multiple décollements. Analogue models and natural examples from the Northern Apennines (Italy). J. Struct. Geol. 28, 185–199.

Milsom, J., Holt, R., Ayub, D.B., Smail, R., 1997. Gravity anomalies and deep structural controls at the Sabah–Palawan margin, South China Sea. In: Fraser, A.J., Matthews, S.J., Murphy, R.W. (Eds.), Petroleum Geology of SE Asia, Geological Society of London Special Publication 126. Geological Society of London, pp. 417–427.

Morley, C.K., 2002. A tectonic model for the tertiary evolution of strike-slip faults and rift basins in SE Asia. Tectonophysics 347, 189–215.

Morley, C.K., 2007. Interaction between critical wedge geometry and sediment supply in a deep-water fold belt. Geology 35, 139–142.

Morley, C.K., 2009. Growth of folds in a deep-water setting. Geosphere 5 (2), 59–89.

Morley, C.K., Back, S., Van Rensbergen, P., Crevello, P., Lambiase, J.J., 2003.

Characteristics of repeated detached, Miocene-Pliocene tectonic inversion events, in a large delta province on an active margin, Brunei Darussalam, Borneo. J. Struct. Geol. 25, 1147–1169.

Morley, C.K., King, R.C., Hillis, R.R., Tingay, M.R.P., Backé, G., 2011. Deepwater fold and thrust belt classification, tectonics, structure and hydrocarbon prospectivity: a review. Earth Sci. Rev. 104, 41–91.

Morley, C.K., von Hagke, C., Hansberry, R.L., Collins, A.S., Kanitpanyacharoen, W., King, R., 2017. Review of major shale-dominated detachment and thrust characteristics in the diagenetic zone: Part I, meso- and macro-scopic scale. Earth Sci. Rev. 173, 168–228.

Mustafar, M.A., Simons, W.J.F., Tongkul, F., Satirapod, C., Omar, K.M., Visser, P.N.A.M., 2017. Quantifying deformation in north Borneo with GPS. J. Geodes. 91, 1241–1259.

Rangin, C., Le Pichon, X., Mazzotti, S., Pubellier, M., Chamot-Rooke, N., Aurelio, M., Walpersdorf, A., Quebral, R., 1999. Plate convergence measured by GPS across the Sundaland/Philippine Sea Plate deformed boundary: the Philippines and eastern Indonesia. Geophys. J. Int. 139, 296–316.

Sandal, S.T., 1996. The Geology and Hydrocarbon Resources of Negara Brunei Darussalam (1996 Revision): Brunei Darussalam, Brunei Shell Petroleum Company/ Brunei Museum. Syabas Bandar Seri Begawan 243 pp.

Sapin, F., Pubellier, M., Lahfid, A., Janots, D., Aubourg, C., Ringenbach, J.-C., 2011. Onshore record of the subduction of a crustal salient: example of the NW Borneo Wedge. Terra. Nova 00, 1–9.

Sapin, F., Hermawan, I., Pubellier, M., Vigny, C., Ringenbach, J.-C., 2012. The recent convergence on the NWBorneo Wedge - a crustal-scale gravity gliding evidenced from GPS. Geophys. J. Int. 193, 549–556.

Sapin, F., Hermawan, I., Pubellier, M., Vigny, C., Ringenbach, J.-C., 2013. The recent convergence on the NW Borneo Wedge - a crustal-scale gravity gliding evidenced from GPS. Geophys. J. Int. 193, 549–556.

Schlische, R.W., Groshong Jr., R.H., Withjack, M.O., Hidayah, T.N., 2014. Quantifying the geometry, displacements, and subresolution deformation in thrust-ramp anticlines with growth and erosion: from models to seismic-reflection profile. J. Struct. Geol. 69, 304–319.

Sclater, J.G., Christie, P.A.F., 1980. Continental stretching: an explanation of the post-mid-cretaceous subsidence of the central north sea basin. J. Geophys. Res. 85, 3711–3739.

Simons, W.J.F., Socquet, A., Vigny, C., Ambrosius, B.A.C., Haji Abu, S., Promthong, C., Subarya, C., Sarsito, D.A., Matheussen, S., Morgan, P., Spakman, W., 2007. A decade of GPS in southeast Asia: resolving Sundaland motion and boundaries. J. Geophys. Res. 11, B06420.

Suppe, J., 2007. Absolute fault and crustal strength from wedge tapers. Geology 35, 1127–1130.

Tan, D.N.K., Lamy, J.M., 1990. Tectonic evolution of the NW Sabah continental margin since the late Eocene. Geol. Soc. Malays. Bull. 27, 241–260.

Taylor, B., Hayes, D.E., 1983. Origin and history of the south China sea basin. In: In: Hayes, D.E. (Ed.), The Tectonic and Geologic Evolution of Southeast Asian Seas and Islands Part 2: Geophysical Monograph, vol. 27. American Geophysical Union, Washington, D.C., pp. 23–56.

Tesei, T., Lacroix, B., Collettini, C., 2015. Fault strength in thin-skinned tectonic wedges across the smectite-illite transition: constraints from friction experiments and critical tapers. Geology 43 (10), 923–926.

Tongkul, F., 1994. The geology of Northern Sabah, Malaysia: its relationship to the opening of the South China Sea basin. Tectonophysics 235, 131–137.

Wang, W., Yin, H., Jia, D., Wu, Z., Wu, C., Zhou, P., 2017. Calculating detachment depth and dip angle in sedimentary wedges using the area–depth graph. J. Struct. Geol. https://doi.org/10.1016/j.jsg.2017.11.014.

William, A.G., Lambiase, J.J., Back, S., Jamiran, M.K., 2003. Sedimentology of the Jalan Selaiman and Bukit Melinsung outcrops, western Sabah: is the west crocker formation an analogue for neogene turbidites offshore? Geol. Soc. Malays. Bull. 47, 63–75.

Wiltschko, D.V., Groshong Jr., R.H., 2012. The Chamberlin 1910 balanced section: context, contribution, and critical reassessment. J. Struct. Geol. 41, 7–23.

Further reading

Hall, R., Morley, C.K., 2004. Sundaland basins. In: In: Clift, P. (Ed.), Continent-Ocean Interactions within East Asian Marginal Seas. Geophys. Monogr. Ser, vol. 149. AGU, Washington, D. C, pp. 55–85.